HHS Public Access

Author manuscript

Electrophoresis. Author manuscript; available in PMC 2016 July 01.

Published in final edited form as:

Electrophoresis. 2015 July ; 36(13): 1499–1506. doi:10.1002/elps.201500119.

DIFFERENTIAL DIELECTRIC RESPONSES OF CHONDROCYTE AND JURKAT CELLS IN ELECTROMANIPULATION BUFFERS

Ahmet C. Sabuncu[1,*], **Anthony J. Asmar**[2,3], **Michael W. Stacey**[2], and **Ali Beskok**[1]

[1]Department of Mechanical Engineering, Southern Methodist University, Dallas, VA, 75275, USA

[2]Frank Reidy Research Center for Bioelectrics, Old Dominion University, Norfolk, VA, 23529, USA

[3]Department of Biological Sciences, Old Dominion University, Norfolk, VA, USA

Abstract

Electromanipulation of cells as a label free cell manipulation and characterization tool has gained particular interest recently. However, the applicability of electromanipulation, particularly dielectrophoresis (DEP), to biological cells is limited to cells suspended in buffers containing lower amounts of salts relative to the physiological buffers. One might question the use of low conductivity buffers (LCB) for DEP separation, as cells are stressed in buffers lacking physiological levels of salt. In LCB, cells leak ions and undergo volume regulation. Therefore, cells exhibit time-dependent DEP response in LCB. In this work, cellular changes in LCB are assessed by dielectric spectroscopy, cell viability assay, and gene expression of chondrocytes and Jurkats. Results indicate leakage of ions from cells, increases in cytoplasmic conductivity, membrane capacitance and conductance. Separability factor, which defines optimum conditions for DEP cell separation, for the two cell types is calculated using the cellular dielectric data. Optimum DEP separation conditions change as cellular dielectric properties evolve in LCB. Genetic analyses indicate no changes in expression of ionic channel proteins for chondrocytes suspended in LCB. Retaining cellular viability might be important during dielectrophoretic separation, especially when cells are to be biologically tested at a downstream microfluidic component.

Keywords

Clausius-Mossotti Factor; Dielectrophoretic Separation; Dielectric Spectroscopy; Microfluidics; Chondrocytes

1 Introduction

DEP has long been utilized to characterize and separate biological cells using externally applied electric fields to induce motion [1]. In general, DEP separation of a cell population from a mixture relies on deflection of cell trajectories around an energy well utilizing positive and negative DEP (pDEP and nDEP) forces, where deflected cells can then be

*Corresponding author: Tel.: +1 214 768 3200. Fax: +1 214 768 1473. asabuncu@smu.edu. .

collected in separate reservoirs. While deflection based methods depend on exerting differential forces on cells around an energy well, chromatographic methods such as DEP flow field fractionation depend on the equilibrium of lateral forces including DEP in laminar flow [2]. Although it is known that the use of low conductivity electromanipulation buffers can result in time-dependent changes in cell dielectric properties, the nature of these changes is unknown [2-5]. The use of these special types of buffers, which contain lower amounts of salts and other added ingredients such as glucose and sucrose, is to maintain physiological osmolarity with relatively less polarizability than mediums at physiological ionic strength. These buffers allow for pDEP response, which is necessary for cell separation, and is not possible using conventional physiological buffers [6].

The fields applied to induce particle motion are well below the limit to introduce permanent pores in cell membrane in DEP settings [7]. While various type of cells were shown viable after DEP manipulation [8], long term exposure to low ionic conditions could have adverse effects. The suspension in low ionic conditions causes an imbalance in the chemical gradient across cell membrane to occur, resulting in ionic efflux and cell volume regulation [5, 9]. Therefore, driven by the transport of electrolytes across the cell membrane causing a shift in the membrane potential, cells exhibit time-dependent dielectric properties and DEP responses. In order to limit those changes and keep separation efficiency at the desired limits, separation experiments are generally performed in relatively short time scales (~10 minutes) [2]. Another practical solution is to cross-link cell membrane or cell wall to stabilize the transmembrane transport. DEP separation of viable and non-viable yeast cells was shown to be enhanced when the cells were treated glutaraldehyde [4]. There are studies utilizing nDEP in high conductivity buffers to separate [10, 11] or characterize [3] cells based on the differences in nDEP force. Although this may seem promising, cell separation efficiency is lower, and separation is prone to generate electrothermal flow effects in high conductivity medium [12].

When exploring the time-dependent changes different cells experience, one consideration is the diversity of ion channels expressed. Here, we compare the dielectric responses of chondrocytes and Jurkat cells in low ionic conditions. Chondrocytes are known to express a wide range of ion channels [13]. These ion channels are necessary to cope with the continual fluxes in osmolarity and ionic gradients in its microenvironment [14]. These ion channels are involved in a number of homeostatic processes including regulated volume increase (RVI), regulated volume decrease (RVD), pH shifts, and maintaining its resting membrane potential [15]. However, lymphocytes express a fraction as many ion channels as chondrocytes [16]. Therefore, we hypothesized that chondrocyte cells are able to tolerate the adverse effects of low ionic concentrations contrary to Jurkat cells, and, in turn, exhibit lower fluctuations in crossover frequency (fxo) than those of Jurkat cells. In order to test this hypothesis, the dielectric response and viability of chondrocyte and Jurkat cells are measured in a low conductivity buffer (LCB) at different time points in an hour. The crossover frequencies of these cells are calculated using the acquired dielectric data. Furthermore, gene expression profiles and intracellular Ca imaging are performed in LCB.

2 Materials and Methods

2.1 Microfluidic Design and Layout

A microfluidic chamber was used for impedance measurements consisting of two parallel plate gold electrodes, with a radius of 500 μm, aligned and housed in a PDMS (polydimethylsiloxane) chamber. Details as well as a picture of the device and a schematic of the setup are given the supplementary information (S1.1 and Figure S2.1). For measurements of the cellular impedance and conductivity of LCB, the microelectrodes were interfaced to an Agilent 4294A precision impedance analyzer (Agilent Technologies, Santa Clara, CA, USA) via a BNC port.

2.2 Theory

The dielectric spectra of cell suspensions were fitted to a series of models: the Cole-Cole model, the Maxwell Wagner mixture model, and the double shell model. Electrode polarization was modeled using a constant phase element model. In the double shell model, the relative permittivity of the medium, cytoplasm, and nucleoplasm (80, 60, and 120, respectively) as well as the thicknesses of the cell membrane and nuclear envelope (7 nm and 40 nm, respectively) are set as constants [17]. The details on the size measurement of the cells is given in the supporting information. Cells' nucleus size was previously measured in a study published by the authors [14, 18]. The volume fraction of the cells was measured using hematocrit tubes. Details of the mathematical procedure and biophysical models are given in a previous publication [18]. Cells were measured in triplicates. Cellular dielectric properties were used to calculate the Clausius-Mossotti (CM) factors of the cells, which is given as [19]:

$$f_{CM}=\frac{\varepsilon^*_{\text{cell}}-\varepsilon^*_{med}}{\varepsilon^*_{\text{cell}}+2\varepsilon^*_{med}}, \quad (1)$$

where $\varepsilon^*_{\text{cell}}$ and ε^*_{med} are complex permittivities of the cell and the medium, respectively. Data modeling for additional compartmental measurements were performed as previously published [18]. Additional details can be found in the supplementary information (S1.2). The uncertainty analysis of the measurements is given in the supplementary information (S1.3). Attraction of cells to high field intensity region (positive CM factor) is possible only in buffers having sufficiently lower electrical conductivity. Lower extracellular ionic concentration cause stronger polarization at the cell interior than the cell exterior and collection/isolation of cells at high intensity regions, consequently [19, 20].

2.3 Cell Culture and Preparation

Dielectric spectroscopy experiments were performed on primary costal chondrocytes and a T-cell leukemia-derived Jurkat E6-1 clone cell line (ATCC® TIB-152™, Manassas, VA, USA). The chondrocyte cells were cultured in Chondrocyte Growth Medium (CGM; PromoCell, Heidelberg, GER), and Jurkat cells in RPMI 1640 medium (Atlanta Biologicals, Norcross, GA). RPMI and CGM supplemented with 10% fetal bovine serum from Atlanta Biologicals and PromoCell, respectively. Both mediums were also supplemented with 2 mM

L-glutamine (Gibco/Invitrogen, Carlsbad, CA), 50 IU/ml penicillin (Gibco/Invitrogen), and 50 mg/ml streptomycin (Gibco/Invitrogen) at 37°C with 5% CO2 in air. All the cells were suspended in an isotonic buffer consisting of 229 mM sucrose, 16 mM glucose, 1 μM $CaCl_2$, and 5 mM Na_2HPO_4 in double distilled water (pH 7.4) for the experiments, after a washing step with the isotonic buffer. The measurements were performed directly after the suspension of cells in LCB. The most common medium used for DEP manipulation in the field is an isotonic sucrose/dextrose solution supplemented with minimal amount of salts for buffering (please see supplementary information S1.4), which could justify our selection of LCB.

2.4 Metabolic Assay

The metabolic activity of cells was evaluated using an MTT Cell Proliferation Assay Kit (ATCC) following manufacturer guidelines. In brief, the assay works by adding a yellow tetrazolium reagent which is reduced by dehydrogenase enzymes, yielding a purple formazan dye. The dye can be solubilized by lysing the cells and measured using a spectrophotometer. Due to cell size differences, about 20,000 chondrocytes/well and 100,000 Jurkats/well were cultured in 96 well plates, then treated with different mediums, and evaluated at different time points. All experiments were performed in triplicate. Additional information can be found in the supplementary information on the methods for the cell diameter and trypan blue assay (S1.5), intracellular calcium imaging (S1.6), and PCR analysis (1.7).

3 Results and Discussion

3.1 Cell Diameter Changes in LCB

Cell diameter is measured in LCB at 10 minute intervals for an hour, and in growth medium (Figure S2.2). Chondrocytes maintained a relatively constant cell volume, whereas Jurkat cell diameter decreased in LCB until 20 minutes, and then quickly increased and stabilized by the 30 minute timepoint. Due to the wash step in LCB before measurements are taken, the initial effects on the cells were not observed. When the measurements were taken, a decrease in cell diameter was already present, suggesting that cells undergo osmotic volume regulation in the few minutes after they are suspended in LCB. The mean diameters of chondrocytes and Jurkat cells are 13.8 μm (±2.9) and 9.3 μm (±1.3), respectively, in LCB, while their diameters in their growth media are 16.1 μm (±3.9) and 11.1 μm (±1.5). The cell radius in LCB is used to model the cells dielectric behavior.

3.2 Clausius-Mossotti Factor and Separability Parameter

Cellular dielectric data was obtained at 801 frequency points between 1 kHz and 10 MHz. Dielectric response was measured every 5 minutes for an hour. The CM factors of cells are calculated at each time point. A spline was fitted to the data points, and the fxo is calculated using an algorithm that estimates the zero of the CM function. The crossover frequencies of chondrocytes and Jurkats are plotted in Figure 1. Figure 1 indicates a decrease in the Jurkat fxo over time, while the chondrocyte fxo remained relatively constant between 10 kHz and 70 kHz. The Jurkat fxo decrease from 230 - 330 kHz range to zero in 25 to 55 minutes, and in time the fxo decreased. The overall measurement uncertainty in determining the fxo is

2.76%. Next, the separability parameter corresponding to these two cell lines is calculated. The separability parameter for a cell pair shows at which frequency range the CM factors of these two cells have opposite polarity and the absolute value of their CM factors is above a certain threshold. The parameter for species *1* and *2* is defined as $S_{12}=\left|\left(a_1^3 Re\left(f_{CM,1}\right)-a_2^3 Re\left(f_{CM,2}\right)\right)/N_{12}\right|$, where $N_{12}=1.5\left(a_1^3-a_2^3\right)$, and subscripts 1 and 2 stand for the chondrocytes and the Jurkats, respectively [12]. Therefore, a nonzero separability value indicates the possibility of a DEP separation. A separability parameter matrix was calculated for all possible combinations of dielectric measurement repetitions. Mean and standard deviation of the combinations were calculated.

In Figure 2, the mean separability parameter is plotted for the chondrocyte and Jurkat cell pair at different time points (standard deviations are shown in Figure S2.3). According to our results, while cells are separable at a wide frequency range (20 kHz to 120 kHz) at the initial time point, the separability window narrows with the passage of time. Between 0 and 25 minutes, separation is achievable between 10 to 100 kHz range. After 25 minutes, separation is possible at the 1 to 10 kHz range. At the initial time point, the Jurkat CM factor is negative below 100 kHz. As Jurkats interact with the LCB, their CM factor shifts from negative to positive; while the chondrocyte CM factor remains negative at this range (Figure 3). Consequently, even though the application of a field frequency between 20 kHz to 120 kHz warrants cell separation initially, after 60 minutes of interaction with LCB, the cell separation window shifts to the 1 kHz to 10 kHz range. Temporal changes in the separation condition of cells are mainly due to how the cells respond to low conductivity buffers, which results in changes to their dielectric properties.

3.3 Metabolic Evaluation of Cells Based on Buffer Compositions

In order to explore some of the cellular changes occurring, the metabolic level of cells was tested using an MTT assay. Cells were suspended in different buffers, such as LCB, LCB supplemented with 10% serum (LCBS), LCB supplemented with 10% serum and 20 mM NaCl (LCBSN), PBS (Phosphate Buffered Saline), PBS supplemented with 10% serum (PBSS), and growth medium. Cell metabolism was measured at 5 minute intervals over the course of an hour. The metabolic levels were normalized to the metabolism of cells in growth medium. In Figure 4, the mean (±SD) metabolism of chondrocytes and Jurkats suspended in different media over an hour are shown with the statistical comparisons in Figure S2.4. Cells had a mean (±SD) metabolic level of 18.6% (±5.6%) for chondrocytes and 5.2% (±1.2%) for Jurkats in LCB. The metabolic levels are low due to the lack of stimulating growth factors as well as an ionic imbalance. When 10% serum is added which has growth factors and stimulates the cell metabolism, the levels significantly increased to 72.1% (±45.1%) for chondrocytes and 15.5% (±2.2%) for Jurkats. It is important to note that the large standard deviation in the chondrocyte measurements is due to the metabolism starting low and then increasing sharply over the hour. In order to see if the ionic composition alone has a major impact, we used PBS which yielded levels of 12.4% (±4.9) for chondrocytes and 11.9% (±0.9%) for Jurkats. However, when PBS was supplemented with serum, the metabolic levels increased to 115.9% (±19.7%) in chondrocytes and 48.2% (±10.4%) in Jurkats. In an attempt to see the effect of adding a minimal amount of salt, LCB

was supplemented with 10% serum and 20 mM of sodium. This combination was effective in Jurkat cells, where an increase to 35.1% (±4.9%) was observed, but oddly, chondrocyte cell levels decreased to 12.2% (±3.6%). The decrease in chondrocytes and increase in Jurkats may be due to chondrocytes being dependent on a mix of salts, and the increase in sodium further shifted the ionic imbalance; whereas Jurkats may be more dependent on sodium concentrations. Furthermore, cells resuspended in their growth medium for an hour after previously being incubated in LCB buffer for an hour showed signs of recovery. The displayed metabolic levels of 86.2% (±2.0%) for chondrocytes and 79.6% (±3.4%) for Jurkats suggests that the cells in LCB enter a state of lower metabolism, but do not undergo complete shutdown and cellular death. In a single experiment, the amount of living versus dead cells was measured using a trypan blue exclusion assay (Figure S2.5). Chondrocytes had no noticeable changes in cell death with respect to time, while Jurkats cells showed an increase in dead cells after 30 minutes.

3.4 Cell Dielectrics and Buffer Composition

The dielectric response of Jurkat cells in LCB with serum and NaCl were measured and the crossover frequencies are calculated. The crossover frequencies of Jurkat cells suspended in LCB, LCB supplemented with 10% serum, and LCB supplemented with serum and 20 mM NaCl, with respect to time are shown in the supplementary information (Figure S2.6). The rate of change in fxo differs based on buffer composition. According to the results, cells that are suspended in buffers with increasing ionic conductivity exhibit a decreasing slope with respect to the temporal axis. Interestingly, the fxo of cells suspended in LCB supplemented with serum and NaCl at the initial time point (0.18 S/m extracellular conductivity) is significantly different from those of cells suspended for one hour in LCB which have similar extracellular conductivity likely due to ion leakage from cells. This suggests that the extracellular conductivity is not the sole factor affecting the fxo, but rather cell response to different environments.

Cells undergo dielectric changes when suspended in buffers with low ionic strength. The cell dielectric parameters and extracellular conductivity values were calculated using dielectric measurements and biophysical models outlined in the materials and methods at 5 minute intervals for an hour. Variations in dielectric parameters indicate increases in membrane capacitance (Figure 5.a), conductance (Figure 5.b), and intracellular (Figure 5.c) extracellular conductivity (Figure 5.d) for both of the cells. The variations in the nuclear dielectric parameters are given in the supplementary information (Figure S2.7). The membrane conductance and capacitance increased in both cells, with respect to time, where the membrane capacitance of chondrocytes and Jurkats and increased at almost the same rate (Figure 5.a), while the rate of increase of the membrane conductance of Jurkat cells was 5 to 10 times higher than that of chondrocytes (Figure 5.b). Throughout the time of measuring, chondrocytes maintained a relatively stable cytoplasmic conductivity while the cytoplasmic conductivity of Jurkat cells increased (Figure 5.c). Similar to the membrane capacitance and conductance, both cells experienced increases in extracellular conductivity; however, the rate of extracellular conductivity increase in chondrocytes was slower than that of Jurkat cells (Figure 5.d).

3.5 Cell Ion Mobility in LCB

Physiological and dielectric effects of low conductivity buffers on mammalian cells are not well known except for red blood cells (RBCs) [21-24]. RBCs undergo a series of changes as described in a model by Glaser and Donath when the extracellular ionic conditions are altered [23]. The model predicts cell shrinkage in LCB and a decrease in cytoplasmic conductivity. We observed a reduction in cell diameter for both cell lines. However, we also observed an increase in the cytoplasmic conductivity contrary to the theory for RBCs. This increase might be related to ionic mobility changes due to intracellular structural changes or ion release from organelles.

We examined the effects of LCB on intracellular calcium concentration in chondrocytes (data not published). These experiments could not be performed on Jurkats due to the use of a vacuum perfusion system. Within seconds of interacting with LCB, chondrocytes experienced a ~7-fold mean increase in the concentration of intracellular calcium. The resulting calcium transient had a lifespan of ~5 minutes. This increase is likely due to release from intracellular stores, seeing as the extracellular medium has little calcium present (1 μM $CaCl_2$). While the decrease in the transient was caused by either efflux of calcium from the cell or uptake of calcium back into the intracellular stores. The formation of intracellular calcium is mainly involved in cellular signaling and is likely part of regulating cellular homeostasis [26] when exposed to LCB. Downstream or other ionic mobility changes are likely causing the changes due to the amount of calcium released is too low to account for the observed increase in the cytoplasmic conductivity.

The main ion exported in red blood cells and erythroleukemia cells in LCB is potassium [25, 26]. Transports of chlorine can also occur in combination with potassium leakage to conserve the electroneutrality of the cell interior and exterior. A study of Jurkats' response to osmotic swelling showed chloride channels playing an active role in volume regulation [27]. Chondrocyte volume regulation is known to be tied to the membrane potential and transport of potassium, chlorine, sodium, and calcium [15]. Increases in the cell membrane conductance, with respect to time, were observed independently from cell volume and extracellular conductivity. The membrane conductance in this context does not solely mean the transmembrane conductance, as typically measured in patch clamp studies, but the conductance at the membrane and in its vicinity. Even though the electrical definition of conductance suggests ionic concentration independence, membrane conductance is dependent on intracellular and extracellular ionic concentration through different mechanisms [28-31].

3.6 Ion channel gene expression

The customized ion channel gene array we used looked at ion channel expression channels involved in sodium, calcium, potassium, chlorine, and hydrogen transport. We measured gene expression changes in ion channels following incubation in LCB for one hour. In chondrocytes and Jurkats, we saw no major changes in gene expression (data not shown), suggesting that any ionic changes occurring in cells following interaction with LCB involves pre-existing ion channels. There are a few considerations about the regulation of cell volume and response to varying changes. Chondrocytes are normally subjected to a variety of

extracellular changes and use ions to regulate their volume [15]. Thus, Jurkats may not be as suited to respond to drastic extracellular changes relative to chondrocytes and may account for some of the more stable levels seen in the dielectric properties of chondrocytes.

3.7 Biological Effects on Cell Dielectrics

Our results further indicate that membrane capacitance increases with an increasing extracellular ion concentration, over time, corresponding to the changes in membrane conductance. This condition may have three explanations: the cell electric double layer capacitance increased with elevated extracellular ion concentrations, the cell surface roughens as cells shrink in LCB, or the dielectric constant at the interface between the cell membrane and extracellular medium can increase as cells leak ions outside. The double layer capacitance can reasonably be approximated to be equal to $\varepsilon \kappa A$, where the terms are the relative permittivity of the double layer, inverse of Debye length, and cell surface area, respectively. As the extracellular medium conductivity increases, the Debye length decreases, resulting in a double layer capacitance increase.

The membrane capacitance is roughly equal to the membrane dielectric constant multiplied by the ratio of the membrane surface area to the membrane thickness. As chondrocytes shrink in LCB, and if there is no loss from lipid membrane, the measured capacitance will increase because of relative increase of cell surface area at a smaller cell. However, the presence of blebs, ruffles, folds, microvilli, and other morphological features increase the surface area of cells and, in turn, membrane capacitance. Chondrocyte cells are adherent cells which have ruffles [32], and once they are released from their anchorage in culture flasks, additional wrinkles can appear on their cell surface in LCB [33], which correlates with measured membrane capacitance. Higher membrane capacitance of chondrocyte cells corresponds to lower crossover frequencies than those of Jurkats.

Lastly, a large dielectric constant at the membrane-solution interface might affect the measured capacitance. The cell membrane is mainly composed of a lipid bilayer, where the relative permittivity of the membrane can be estimated between 2 and 5, and the relative permittivity of the external aqueous medium is around 80 at 300K [34, 35]. One would assume that the dielectric constant will vary smoothly between the aqueous medium and lipid bilayer, as the dielectric constant of water in the interphase region will have values lower than 80 [36]. A previous study showed the dielectric constant having values of 10-70 measured at this interfacial region using dielectric probes [37]. Furthermore, molecular dynamics simulations of lipid membrane-water complexes indicated a large dielectric constant at the lipid-water interface, where the dielectric constant at this region is several times higher than the dielectric constant of water [38]. The large dielectric constant at this region is considered to be due to presence of oppositely charged head groups in the membrane lipids, namely choline and phosphate groups. The dielectric constant at this region can further be amplified if counter ions accumulate at the interface generating a second high dielectric layer. Perhaps, in the view of this discussion, it is more realistic to model the cell membrane as three dielectric slabs in series rather than single one. In this way, it will be possible to account for capacitance increments induced by ion accumulation at the membrane-water interface.

4 Conclusions

Here, we compared DEP responses of chondrocyte and Jurkat cells, which are known to have different number and diversity of ion channels [14]. While chondrocytes exhibited relatively stable fxo values, the Jurkats had a decreasing trend over time. We showed that the variations in fxo impact DEP cell separation by plotting the separability parameter for these cells as a function of time. As cells exhibit time-dependent changes in LCB, the optimal separability conditions change. This could be true for other cell lines; however, future tests with different cell types, including bacteria and yeast, are needed to elucidate their time-dependent DEP responses. While the addition of serum and electrolytes can increase cellular viability during separation, long term (~30 minutes) exposure to LCB should be avoided in DEP experiments. Though, if the cell viability is not an issue, cells could be fixed (for instance with formaldehyde) prior to DEP separation. Furthermore, separation systems could be developed that utilize small changes in nDEP responses of cells in high conductivity buffers.

Overall, Jurkat cells are intrinsically adapted to live in a nutrient rich and osmotically stable blood environment, whereas chondrocyte cells are naturally exposed to gradients of extracellular pH, ionic concentration, and osmolarity in cartilage. The changing environment of chondrocyte cells may explain their relative tolerance to low ionic concentration. Overall, the use of LCB incurs cell-specific, time-dependent cellular responses leading to shifts in the fxo necessary for DEP separation.

Supplementary Material

Refer to Web version on PubMed Central for supplementary material.

Acknowledgements

Research reported in this publication was supported by the National Institute of Arthritis and Musculoskeletal and Skin Diseases of the National Institute of Health under the award number R21AR063334. The content is solely the responsibility of the authors and does not necessarily represent the views of the NIH.

References

[1]. Çetin B, Li D. Electrophoresis. 2011; 32:2410–2427. [PubMed: 21922491]

[2]. Gascoyne PR, Noshari J, Anderson TJ, Becker FF. Electrophoresis. 2009; 30:1388–1398. [PubMed: 19306266]

[3]. Gielen F, deMello AJ, Edel JB. Analytical Chemistry. 2011; 84:1849–1853.

[4]. Gagnon Z, Mazur J, Chang H-C. Biomicrofluidics. 2009; 3:0441081–11.

[5]. Lin RZ, Ho CT, Liu CH, Chang HY. Biotechnology journal. 2006; 1:949–957. [PubMed: 16941445]

[6]. Gascoyne, PR. Field-Flow Fractionation in Biopolymer Analysis. Williams, S.; Kim, R.; Caldwell; Karin, D., editors. Springer; Vienna: 2012. p. 255-275.

[7]. Menachery A, Pethig R. Nanobiotechnology, IEE Proceedings, IET. 2005:145–149.

[8]. LaLonde A, Romero-Creel MF, Lapizco-Encinas BH. Electrophoresis. 2014 in print, DOI: 10.1002/elps.201400331.

[9]. Gurtovenko AA, Vattulainen I. The Journal of Physical Chemistry B. 2007; 111:13554–13559.

[10]. Park S, Zhang Y, Wang T-H, Yang S. Lab on a Chip. 2011; 11:2893–2900. [PubMed: 21776517]

[11]. Park S, Koklu M, Beskok A. Analytical chemistry. 2009; 81:2303–2310.
[12]. Sabuncu AC, Beskok A. Electrophoresis. 2013; 34:1051–1058. [PubMed: 23348751]
[13]. Barrett-Jolley R, Lewis R, Fallman R, Mobasheri A. Frontiers in physiology. 2010; 1:1–11. [PubMed: 21522484]
[14]. Stacey MW, Sabuncu AC, Beskok A. Biochimica et Biophysica Acta (BBA)-General Subjects. 2014; 1840:146–152. [PubMed: 24016606]
[15]. Lewis R, Feetham CH, Barrett-Jolley R. Cellular Physiology and Biochemistry. 2011; 28:1111–1122. [PubMed: 22179000]
[16]. Feske S, Skolnik EY, Prakriya M. Nature Reviews Immunology. 2012; 12:532–547.
[17]. Ermolina I, Polevaya Y, Feldman Y, Ginzburg B-Z, Schlesinger M. Dielectrics and Electrical Insulation, IEEE Transactions on. 2001; 8:253–261.
[18]. Sabuncu AC, Zhuang J, Kolb JF, Beskok A. Biomicrofluidics. 2012; 6:0341031–15.
[19]. Jones, TB.; Jones, TB. Electromechanics of particles. Cambridge University Press; Cambridge: 2005.
[20]. Gascoyne PR, Shim S. Cancers. 2014; 6:545–579. [PubMed: 24662940]
[21]. Gimsa J, Schnelle T, Zechel G, Glaser R. Biophysical journal. 1994; 66:1244–1253. [PubMed: 8038395]
[22]. Glaser R. The Journal of membrane biology. 1982; 66:79–85. [PubMed: 7077650]
[23]. Glaser R, Donath J. Bioelectrochemistry and Bioenergetics. 1984; 13:71–83.
[24]. Bernhardt I, Hall A, Ellory J. The Journal of physiology. 1991; 434:489–506. [PubMed: 2023127]
[25]. Gascoyne PR, Pethig R, Burt JP, Becker FF. Biochimica et Biophysica Acta (BBA)-Biomembranes. 1993; 1149:119–126. [PubMed: 8318523]
[26]. Georgiewa R, Donath E, Gimsa J. Journal of electroanalytical chemistry and interfacial electrochemistry. 1989; 276:255–270.
[27]. Ross PE, Garber SS, Cahalan MD. Biophysical journal. 1994; 66:169–178. [PubMed: 8130336]
[28]. Lyklema J. Journal of Physics: Condensed Matter. 2001; 13:5027–5034.
[29]. McLaughlin S, Szabo G, Eisenman G, Ciani S. Proceedings of the National Academy of Sciences. 1970; 67:1268–1275.
[30]. Donath E, Egger M, Pastushenko VP. Journal of Electroanalytical Chemistry and Interfacial Electrochemistry. 1990; 298:337–360.
[31]. Lewis C. The Journal of Physiology. 1979; 286:417–445. [PubMed: 312319]
[32]. Guilak F, Erickson GR, Ting-Beall HP. Biophysical journal. 2002; 82:720–727. [PubMed: 11806914]
[33]. Gascoyne PR, Shim S, Noshari J, Becker FF, Stemke-Hale K. Electrophoresis. 2013; 34:1042–1050. [PubMed: 23172680]
[34]. Pethig, R. Dielectric and Electronic Properties of Biological Materials. John Willey & Sons; New York: 1979.
[35]. Kaatze U. Journal of Chemical and Engineering Data. 1989; 34:371–374.
[36]. Ashcroft R, Coster H, Smith J. Biochimica et Biophysica Acta (BBA)-Biomembranes. 1981; 643:191–204. [PubMed: 7236687]
[37]. Cevc G. Biochimica et Biophysica Acta (BBA)-Reviews on Biomembranes. 1990; 1031:311–382. [PubMed: 2223819]
[38]. Nymeyer H, Zhou H-X. Biophysical journal. 2008; 94:1185–1193. [PubMed: 17951302]

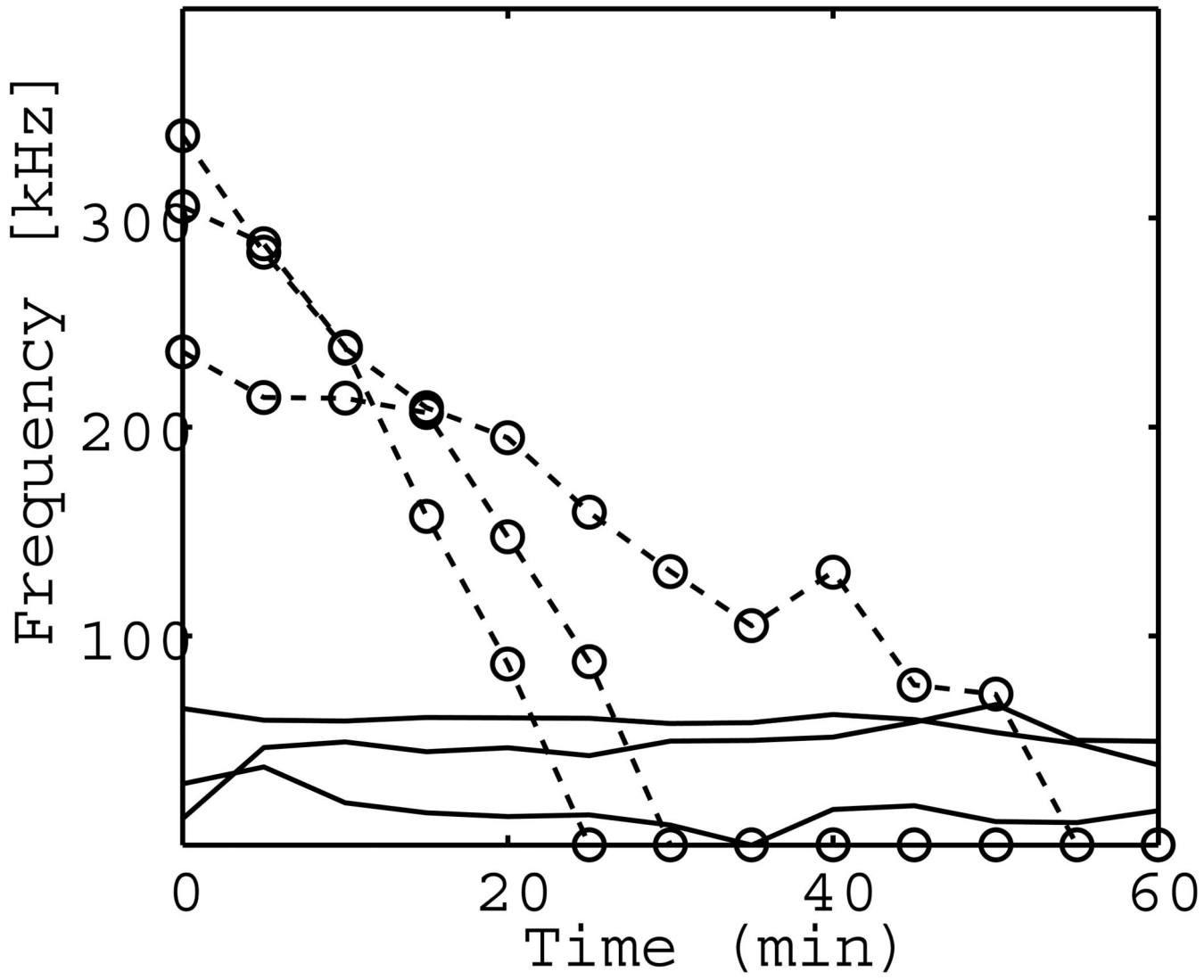

Figure 1.

Temporal changes of DEP crossover frequency and separability. Time-dependent evolution of DEP crossover frequency for chondrocyte (solid line) and Jurkat (dashed line) cells in low conductivity buffer. The conductivity of the buffer is 0.06 S/m.

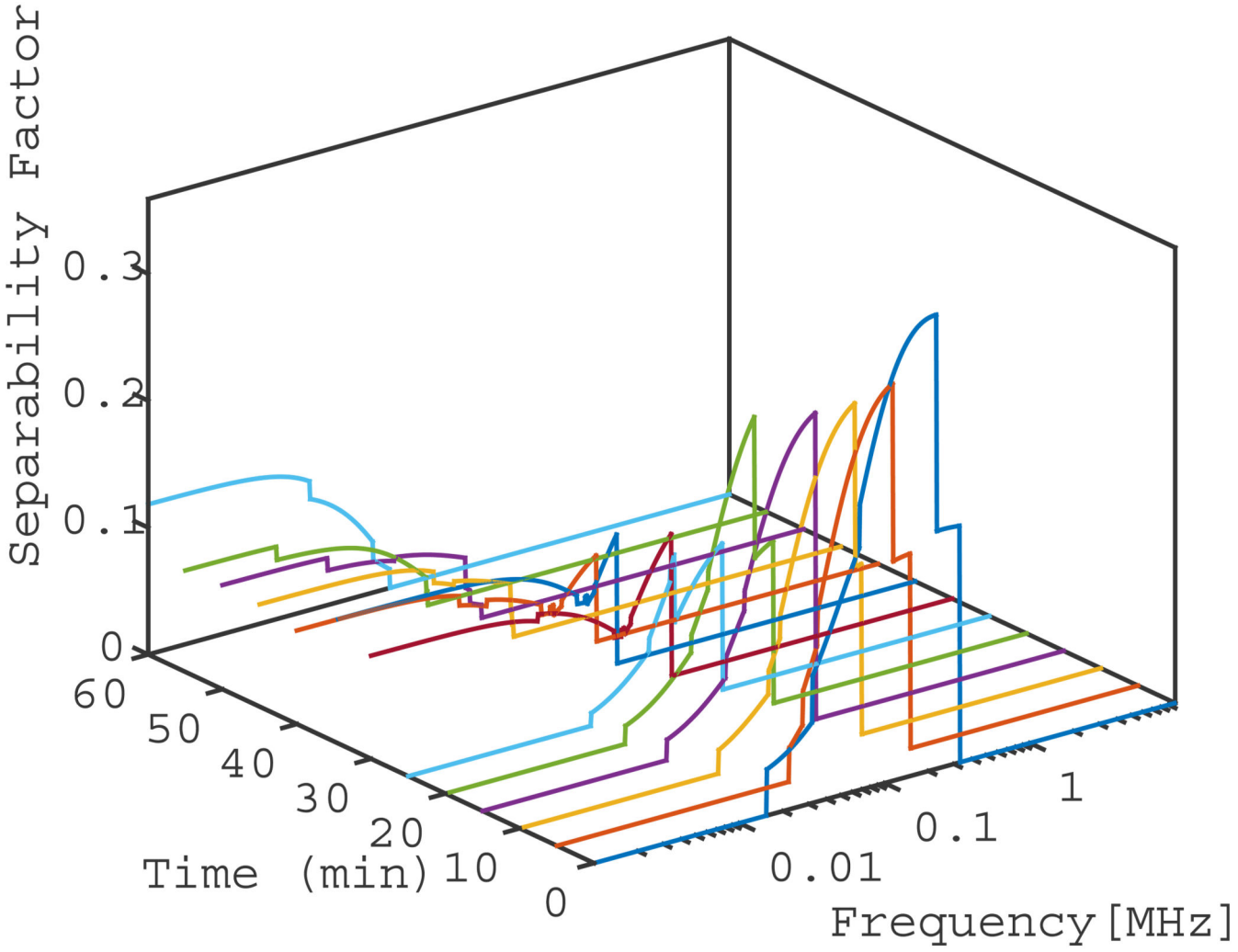

Figure 2.
Time evolution of the mean separability parameter of the chondrocyte–Jurkat cell pair in low conductivity buffer. The conductivity of the buffer is 0.06 S/m.

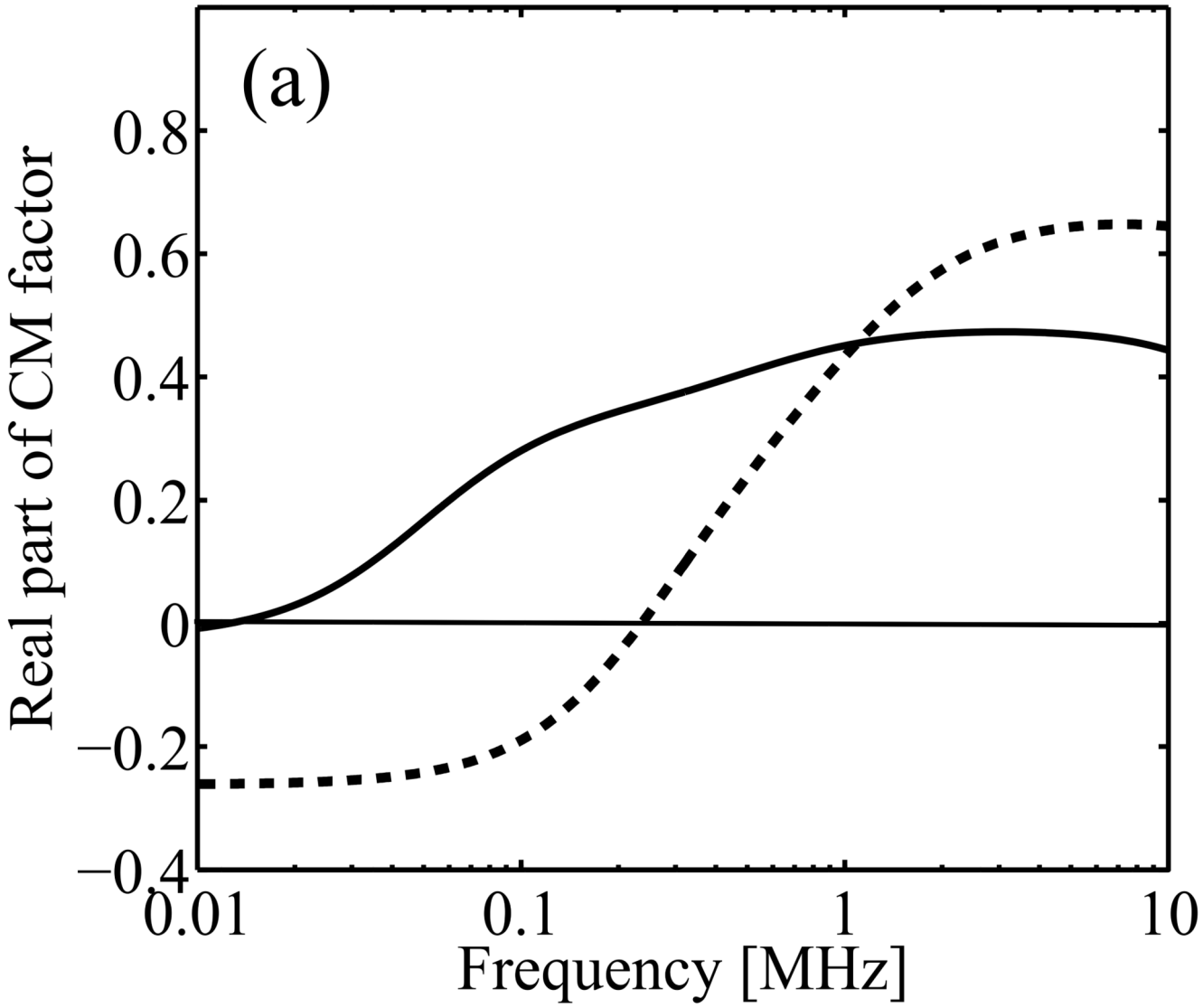

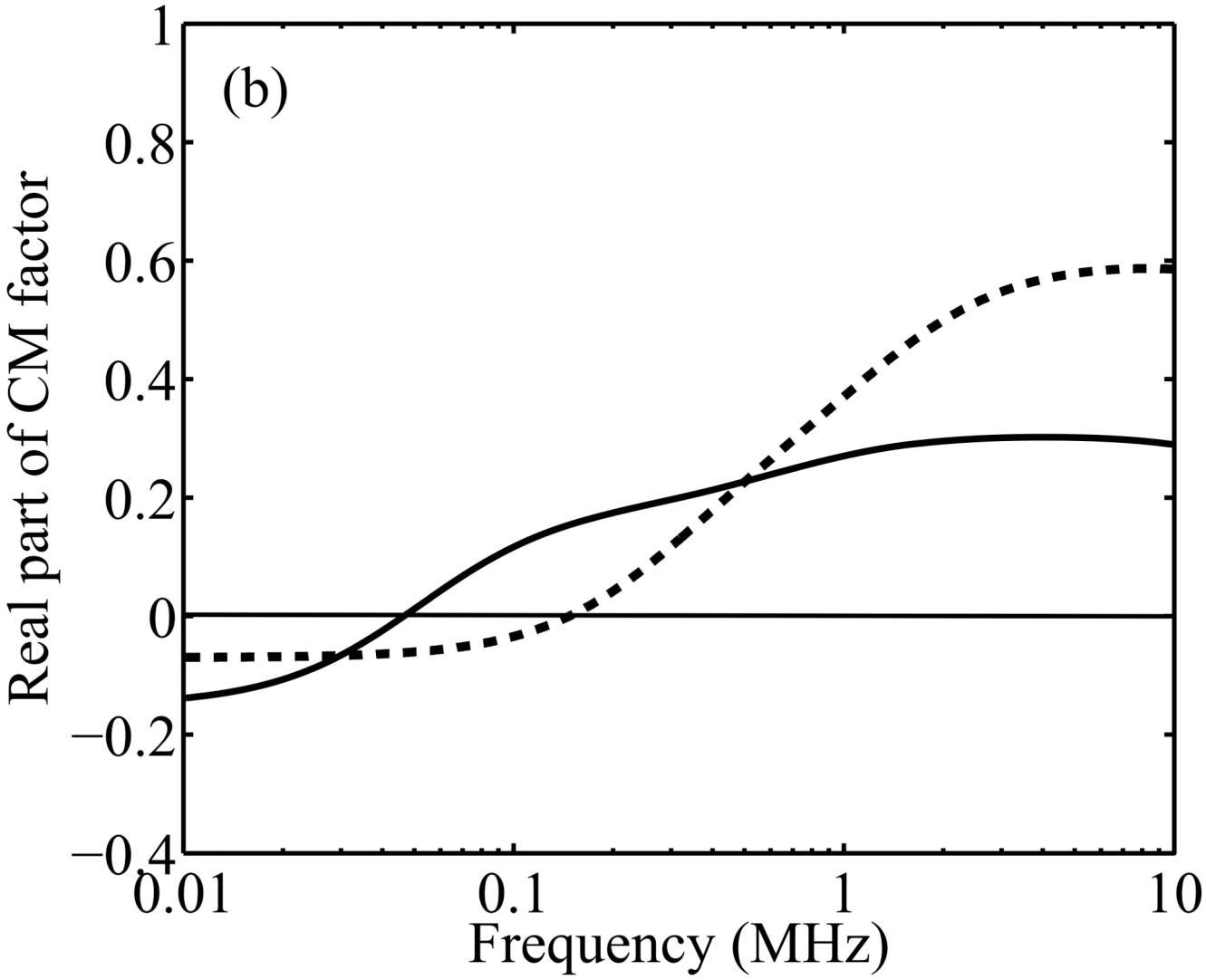

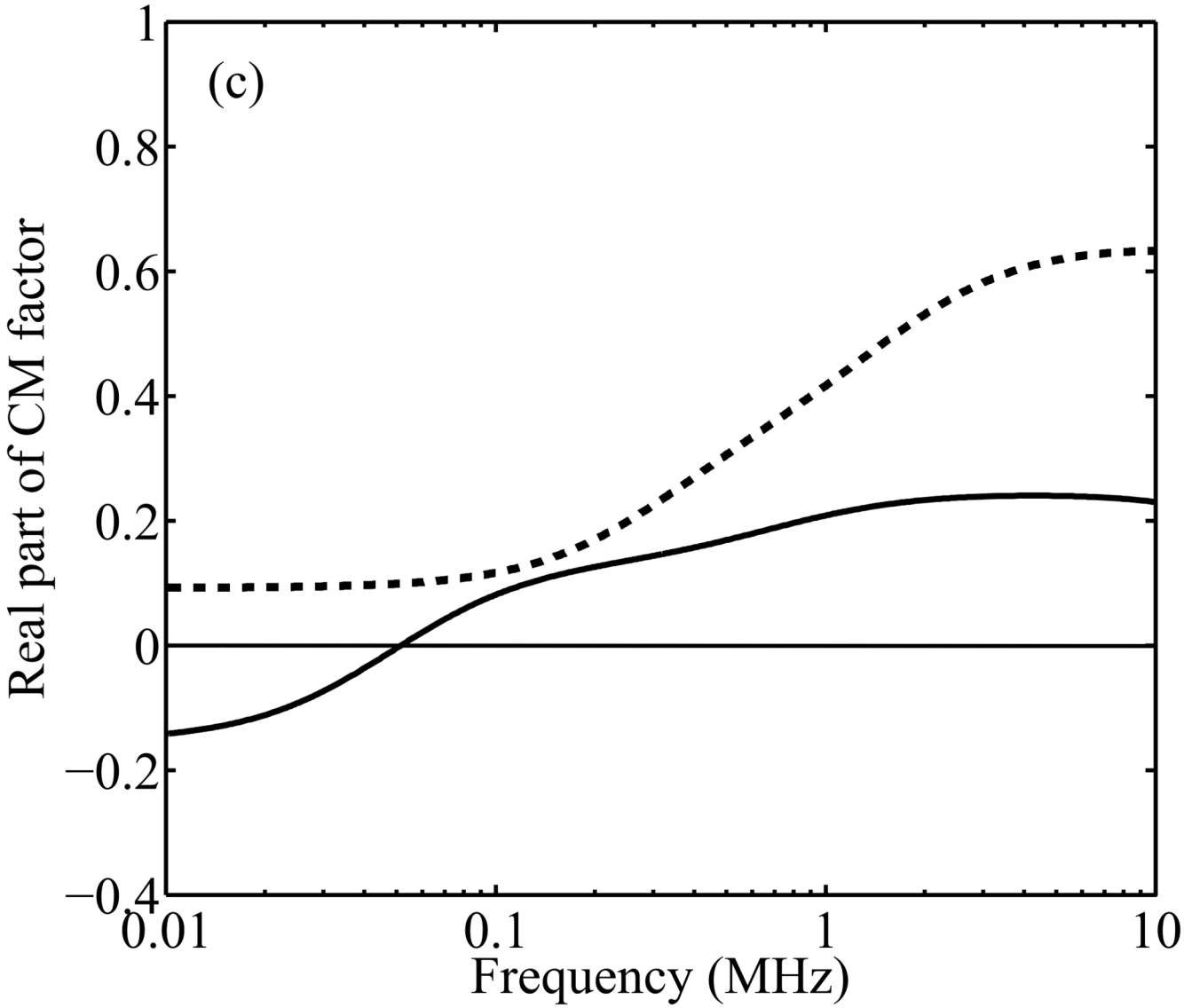

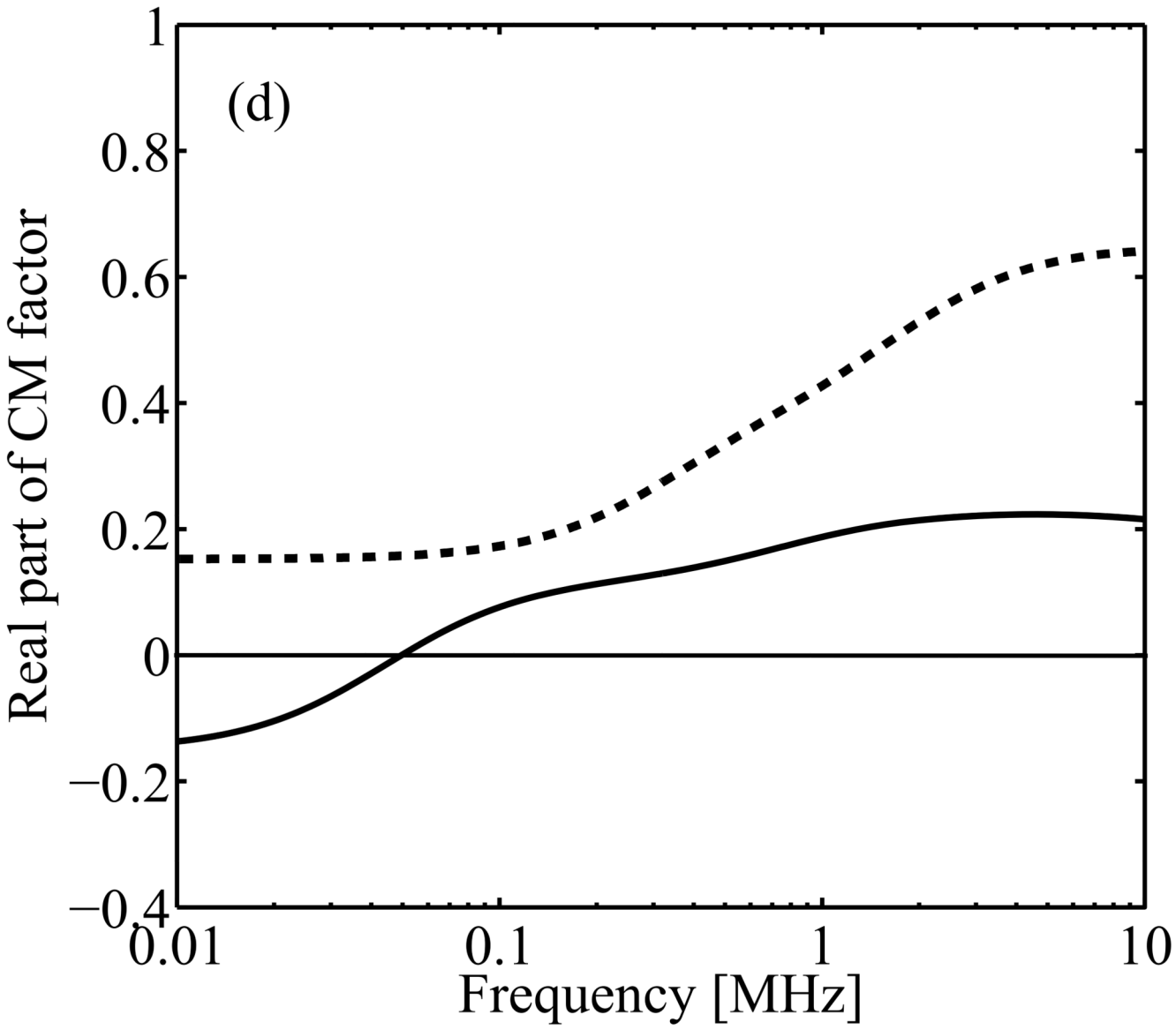

Figure 3.

Clausius-Mossotti factors of chondrocyte (solid line) and Jurkat (dashed line) cells at initial time point (a), 20 minutes (b), 40 minutes (c), and at 60 minutes (d). The conductivity of the buffer is 0.06 S/m.

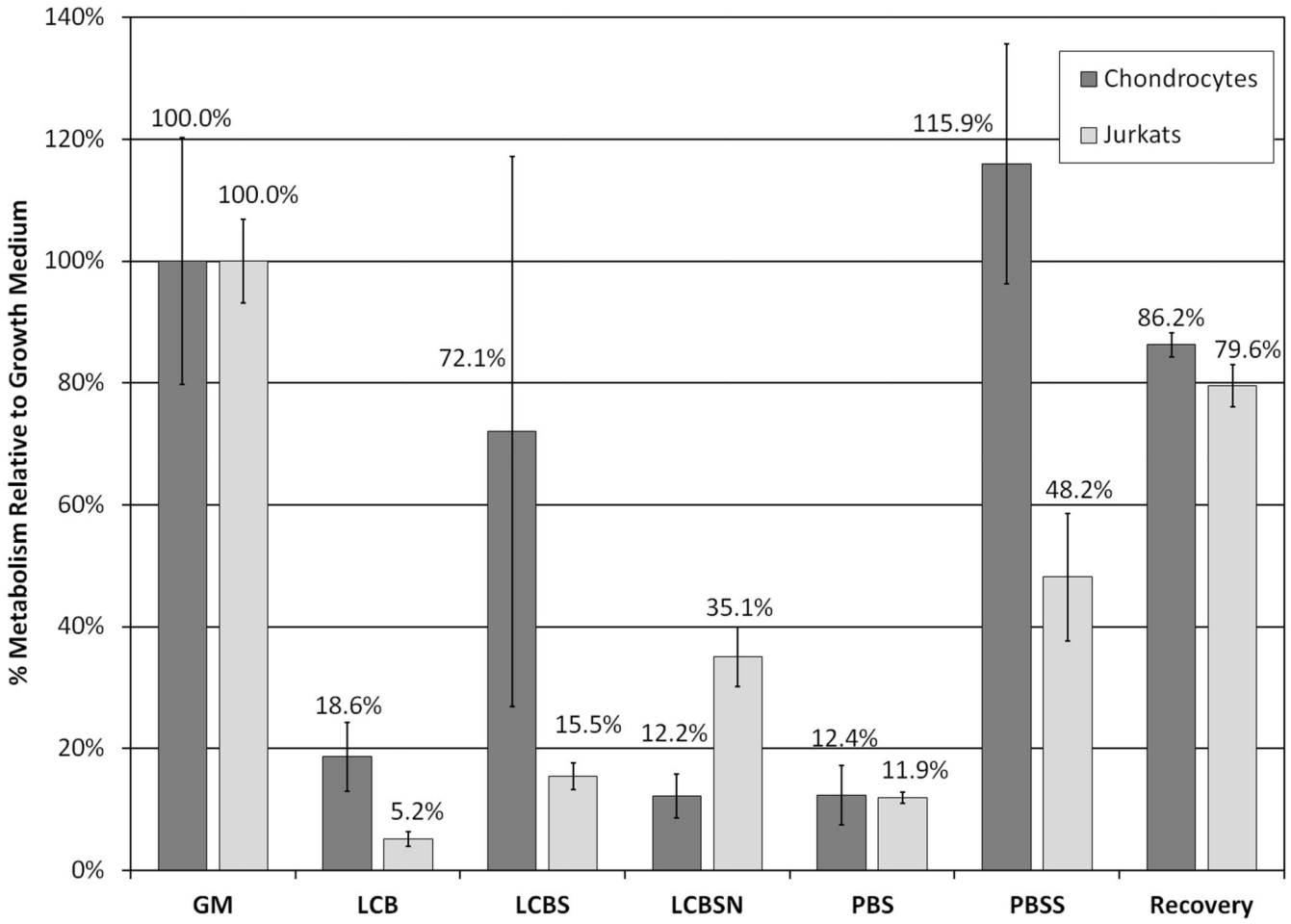

Figure 4.

Metabolic activity of chondrocyte and Jurkat cells in different solutions relative to growth medium. Cells were grown for an hour in low conductivity buffer (LCB), LCB with 10% serum (LCBS), LCBS with 20mM NaCl (LCBSN), phosphate buffered saline (PBS), and PBS with 10% serum (PBSS). Cells in LCB were additionally incubated for 1 hour in growth medium (recovery).

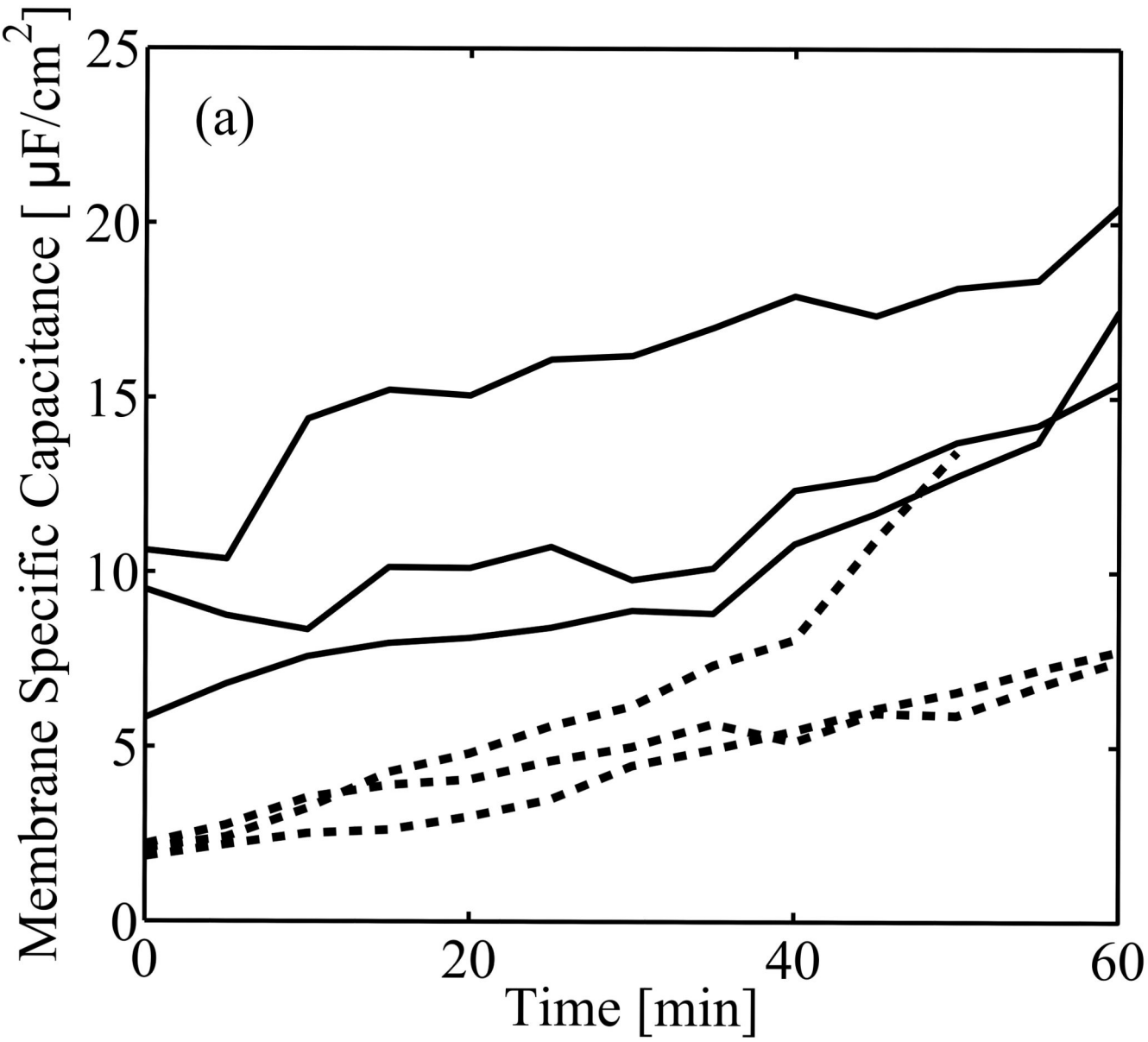

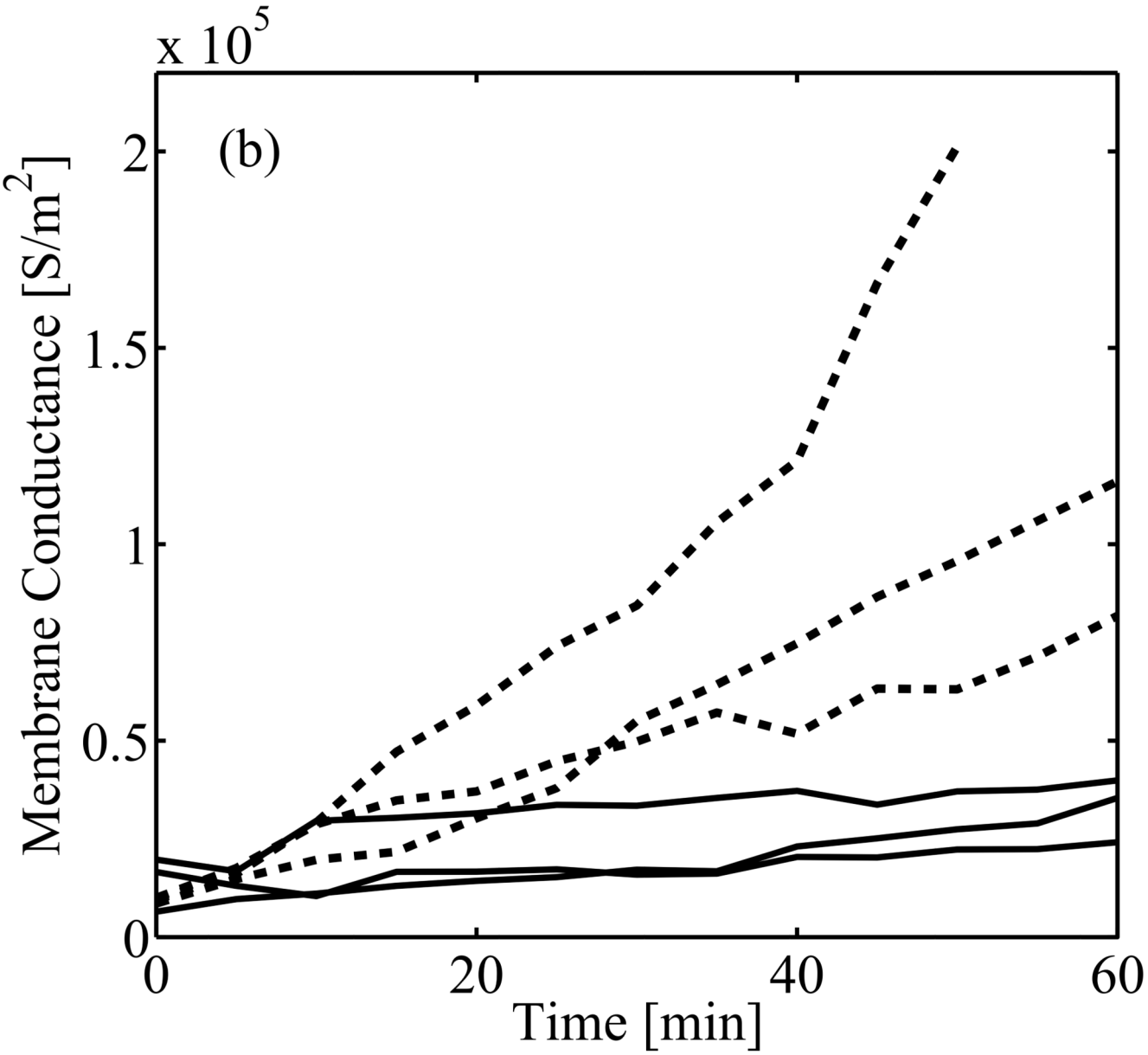

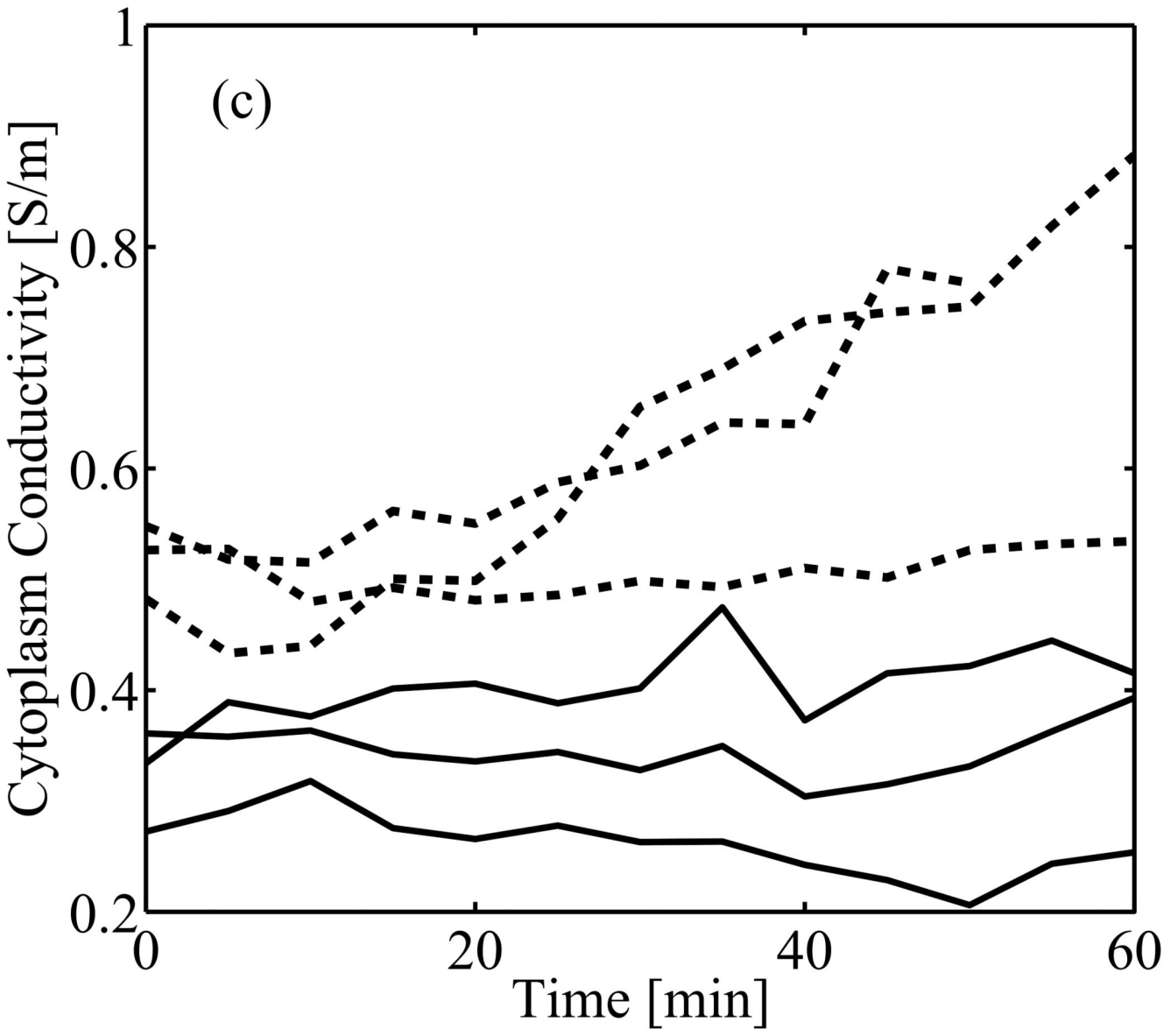

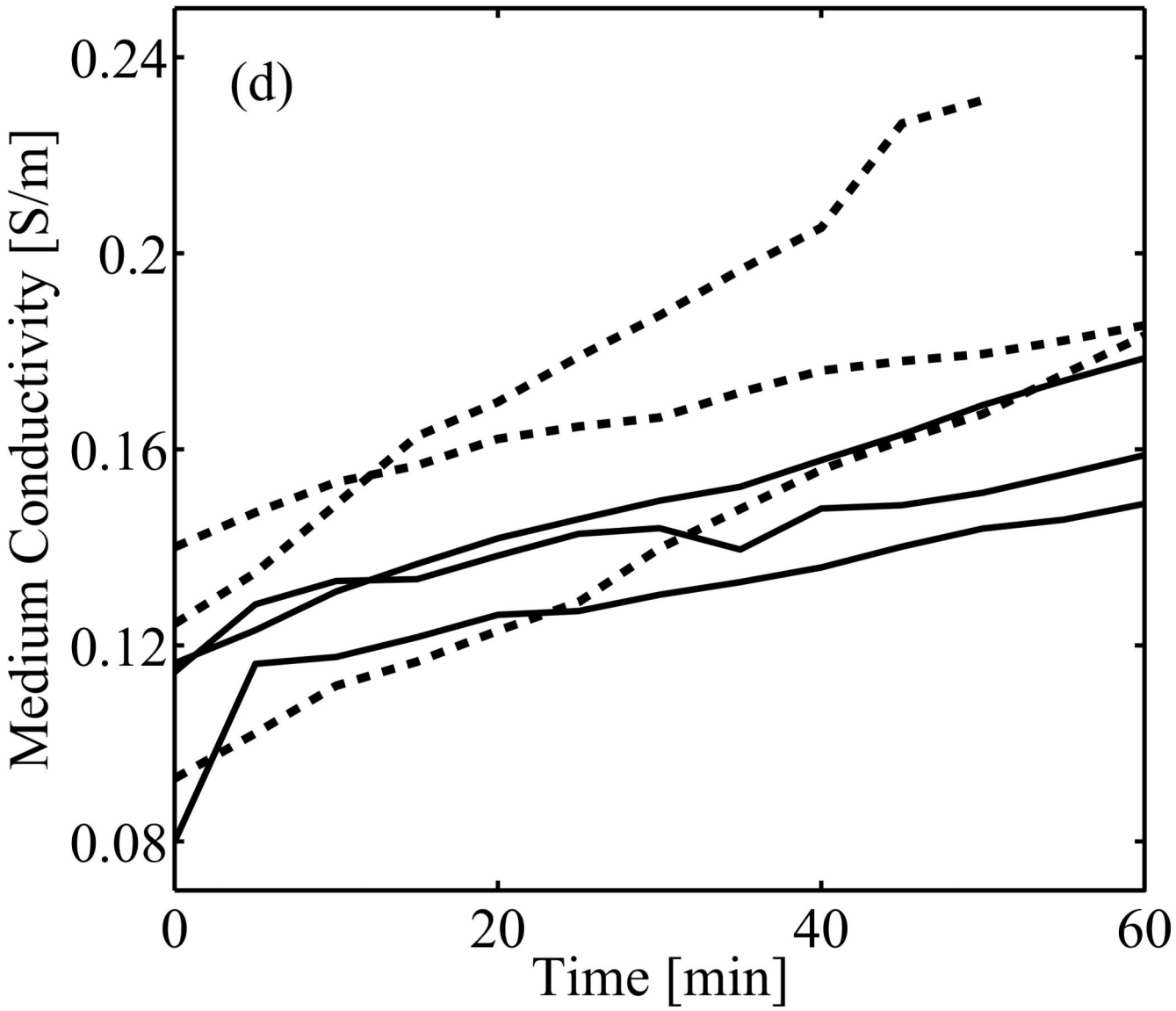

Figure 5.

Evolution of the dielectric properties of chondrocytes (solid line) and Jurkat (dashed) cells with time. All repetitions are presented in the figures. In (d) extracellular conductivity changes of Jurkat (dashed line) and chondrocyte (solid line) cells suspended in LCB are shown. The conductivity of the buffer is 0.06 S/m.